THE JOURNAL OF BIOLOGICAL CHEMISTRY VOL. 288, NO. 23, pp. 16348–16360, June 7, 2013
© 2013 by The American Society for Biochemistry and Molecular Biology, Inc. Published in the U.S.A.

MicroRNA-33a Mediates the Regulation of High Mobility Group AT-Hook 2 Gene (*HMGA2*) by Thyroid Transcription Factor 1 (TTF-1/NKX2–1)*[S]

Received for publication, April 3, 2013, and in revised form, April 24, 2013 Published, JBC Papers in Press, April 26, 2013, DOI 10.1074/jbc.M113.474643

Shawn J. Rice[‡], Shao-Chiang Lai[§¶], Lauren W. Wood[§¶], Kaitlin R. Helsley[§¶], E. Aaron Runkle[‖], Monte M. Winslow[**], and David Mu[§¶1]

*From the [‡]Penn State Cancer Institute, Penn State University, Hershey, Pennsylvania 17033, the [§]Leroy T. Canoles Jr. Cancer Research Center, Eastern Virginia Medical School, Norfolk, Virginia 23501, the [¶]Department of Microbiology and Molecular Cell Biology, Eastern Virginia Medical School, Norfolk, Virginia 23501, the [‖]Department of Pathology, University of Pennsylvania, Philadelphia, Pennsylvania 19104, and the **Department of Genetics, Stanford University School of Medicine, Stanford, California 94305*

Background: *TTF-1* inhibits lung cancer progression via *HMGA2* down-regulation.
Results: *TTF-1* up-regulates miR-33a, which in turn directly represses *HMGA2*.
Conclusion: The signaling axis of *TTF-1* to *HMGA2*, important in controlling lung cancer metastasis, is mediated by miR-33a.
Significance: This study explains the mechanism of *HMGA2* suppression by *TTF-1*.

In lung cancers, *TTF-1* displays seemingly paradoxical activities. Although *TTF-1* is amplified in primary human lung cancers, it inhibits primary lung tumors from metastasizing in a mouse model system. It was reported that the oncogenic proepithelial mesenchymal transition (EMT) high mobility group AT-hook 2 gene (*HMGA2*) mediates the antimetastatic function of *TTF-1*. To gain mechanistic insight into the metastasis-critical signaling axis of *TTF-1* to *HMGA2*, we used both reverse and forward strategies and discovered that microRNA-33a (miR-33a) is under direct positive regulation of *TTF-1*. By chromatin immunoprecipitation, we determined that TTF-1 binds to the promoter of *SREBF2*, the host gene of miR-33a. The 3′-untranslated region (UTR) of *HMGA2* contains three predicted binding sites of miR-33a. We showed that the first two highly conserved sites are conducive to *HMGA2* repression by miR-33a, establishing *HMGA2* as a genuine target of miR-33a. Functional studies revealed that enforced expression of miR-33a inhibits the motility of lung cancer cells, and this inhibition can be rescued by overexpression of the form of *HMGA2* without the 3′-UTR, suggesting that *TTF-1* keeps the prometastasis gene *HMGA2* in check via up-regulating miR-33a. This study reports the first miRNAs directly regulated by *TTF-1* and clarifies how *TTF-1* controls *HMGA2* expression. Moreover, the documented importance of *SREBF2* and miR-33a in regulating cholesterol metabolism suggests that TTF-1 may be a modulator of cholesterol homeostasis in the lung. Future studies will be dedicated to understanding how miRNAs influence the oncogenic activity of TTF-1 and the role of TTF-1 in cholesterol metabolism.

MicroRNAs (miRNAs)[2] are small RNAs that do not encode proteins (1–4). The biological consequences of microRNA expression perturbation are manifested by a wide range of cellular or organismal phenotypes, including cancers (2). In the lung, miRNAs play critical roles in both development and tumorigenesis (5–8). Over 100 miRNAs are dynamically regulated during organogenesis of a normal murine lung (9). Selected examples of miRNAs influencing lung development include miR-17∼92, as evidenced by the lung developmental defect in the knock-out mice (10), and miR-302/367, which regulates lung endoderm (11). The better characterized let-7 miRNA family also shows decreased expression in advanced lung cancers (12). Let-7s target a number of oncogenes, including *HMGA2* (13–15). The let-7-directed repression of *HMGA2* is robust, probably due to the fact that the 3-kb *HMGA2* 3′-UTR contains seven let-7 binding sites. Human tumor-associated gene translocation of *HMGA2* eliminates its 3′-UTR, thus liberating *HMGA2* from the let-7-directed repression (13, 14).

Despite advancements in our understanding of the miRNA biology in lung cancer (16), the extent of the interconnection between miRNA-based networks and critical lung cancer genes remains poorly characterized. In this regard, we focus on a master regulator of the lung developmental transcription program termed thyroid transcription factor 1 (*TTF-1* or *NKX2–1*). In addition to being indispensable to fetal lung organogenesis and morphogenesis (17), *TTF-1* also contributes to adult lung tumorigenesis based on the genetic evidence that *TTF-1* is part of a recurrent multigenic amplicon in lung cancers (18–21). Subsequent studies have identified *ROR1* and *LMO3* as indispensable downstream mediators of *TTF-1* in lung adenocarcinomas (22, 23). Seemingly at odds with the observation that *TTF-1* is a lung oncogene, *Ttf-1* was also found to prevent primary lung adenocarcinomas from metastasizing in a mouse model system (24). Moreover, a loss of the *Ttf-1* allele cooper-

* This work was supported, in whole or in part, by National Institutes of Health, NCI, Grant CA127547 (to D. M.).
[S] This article contains supplemental Table 1.
[1] To whom correspondence should be addressed: Leroy T. Canoles Jr. Cancer Research Center, Department of Microbiology and Molecular Cell Biology, Eastern Virginia Medical School, Norfolk, VA 23501. E-mail: mud@evms.edu.

[2] The abbreviations used are: miRNA, microRNA; QPCR, quantitative real-time PCR; LNA, locked nucleic acid; dox and Dox, doxycycline.

ates with oncogenic $Kras^{G12D}$, causing pulmonary tumors in transgenic mice that were phenotypically similar to human mucinous adenocarcinomas (25, 26). In view of the multifaceted activities of TTF-1 in lung biology, we believe that mapping the connections between the miRNA network and the TTF-1-directed transcriptional program would provide novel entry points to investigate the lung biology orchestrated by TTF-1. To this end, we have recently reported the discovery of the first miRNA (*i.e.* miR-365) that directly regulates *TTF-1* expression via binding to the *TTF-1* 3′-UTR (27). In this study, we concentrate on searching for the miRNAs acting downstream to TTF-1 and have uncovered multiple microRNAs that are directly regulated by TTF-1. One such miRNA, miR-33a, was chosen for a comprehensive characterization in view of the fact that it scored in both reverse and forward screens. The results unambiguously place miR-33a under the positive transcriptional control of TTF-1. Moreover, we discovered that the *HMGA2* oncogene, known to be repressed by TTF-1 (24), is a direct target repressed by miR-33a. Loss- and gain-of-function analyses validate miR-33a as a mediator of the *HMGA2* repression by TTF-1 (TTF-1 → miR-33a ⊣ HMGA2). In light of our observations, we believe that TTF-1 utilizes miR-33a as a means to abate *HMGA2* expression. Considering the known activities of miR-33a outside of cancer biology (*e.g.* cholesterol metabolism (28)), the results of this study are expected to carve out novel directions for future research on TTF-1-orchestrated lung biology.

EXPERIMENTAL PROCEDURES

Cell Culture and Expression Vectors—The human lung cancer cell lines NCI-H358, NCI-H441, A549, NCI-H1299, and BEAS-2B were acquired from the American Type Culture Collection (ATCC), and maintained as described previously (29). Mouse 394T4-bc37 (shLuc) and 394T4-E1 (shTtf-1) cells were provided by Dr. Monte Winslow (24) and maintained in DMEM supplemented with 10% fetal bovine serum, penicillin, and streptomycin. The pGL4.10 *SPB* promoter reporter construct and pcDNA3.1 *TTF-1* and *TTF-1* homeodomain deletion mutant expression vectors were constructed previously (29). The *SREBF2* (−998 to −3, relative to the transcription start site) and *C9ORF5* (−1000 to −5) promoters were PCR-amplified from human genomic DNA using primers listed in Table 1 and cloned into the promoterless luciferase vector pGL4.10 Basic (Promega). Deletion mutants of miR-33a binding sites were derived from a psiCHECK2 vector containing the 3′-UTR of *HMGA2* fused to the 3′-end of a *Renilla* luciferase gene, kindly provided by Dr. Marcus Peter (30). Mutation constructs were created using the QuikChange site-directed mutagenesis kit (Stratagene) according to the manufacturer's protocol; the primers are listed in Table 1. The human *HMGA2* cDNA expression plasmid was obtained from Dr. Jian-Jun Wei (31), and the murine *Hmga2* cDNA was from Addgene (Cambridge, MA).

RNA Oligonucleotide Reagents and Transfection—All siRNAs, miRNA mimics, and inhibitors were purchased from Dharmacon. Cells were transiently transfected with plasmid DNA, siRNA (non-targeting negative control, D-001210-01; TTF-1 A/B/C, D019105–03/04/17), antisense oligonucleotide miRNA inhibitors (non-targeting negative control, IN-001001–01; hsa-miR-33a inhibitor, IH-300509–08), or miRNA mimics (non-targeting control, CN-001005–01; hsa-miR-33a (C-300509–07) using Lipofectamine 2000 (Invitrogen) according to the manufacturer's protocol. Transfection efficiency was monitored with pMAXGFP plasmid or BLOCK-iT fluorescently labeled negative control oligonucleotides (Invitrogen) and judged to be >90% for each cell line.

RNA Isolation and Reverse Transcription (RT)-Quantitative Real-time PCR (QPCR) Analysis—Total RNA (miRNA and mRNA) was isolated from cells using TRIzol (Invitrogen). For mRNA quantification, RNA was reverse transcribed using the High Capacity cDNA synthesis kit (Applied Biosystems). The resultant cDNA was evaluated by real-time PCR using the primers listed in Table 1 and Brilliant II SYBR Green master mix (Stratagene) with a StepOne Plus real-time PCR system (Applied Biosystems). MicroRNAs were quantified using miRCURY™ (Exiqon) or qScript (Quanta Biosciences) miRNA cDNA synthesis kits followed by real-time PCR analysis using locked nucleic acid (LNA) miRNA-specific PCR primers and miRCURY™ SYBR Green master mix (Exiqon) or PerfeCta miRNA assays and PerfeCta SYBR Green master mix (Quanta Biosciences), respectively.

MicroRNA Array Profiling—Total RNA was harvested for profiling using the Cell and Plant miRCURY™ RNA isolation kit (Exiqon). The quality of the total RNA was verified by an Agilent 2100 bioanalyzer profile. Total RNA (700 ng) from sample and reference was labeled with Hy3™ and Hy5™ fluorescent label, respectively, using the miRCURY™ LNA Array power labeling kit (Exiqon) following the procedure described by the manufacturer. The Hy3™-labeled samples and a Hy5™-labeled reference RNA sample were mixed pairwise and hybridized to the miRCURY™ LNA Array version 5th Generation (Exiqon), which contains capture probes targeting all miRNAs for humans, mice, or rats registered in miRBASE version 16.0 at the Sanger Institute. The hybridization was performed according to the miRCURY™ LNA array manual using a Tecan HS4800 hybridization station. After hybridization, the microarray slides were scanned and stored in an ozone-free environment (ozone level below 2.0 ppb) in order to prevent potential bleaching of the fluorescent dyes. The miRCURY™ LNA array microarray slides were scanned using the Agilent G2565BA microarray scanner system (Agilent Technologies), and the image analysis was carried out using ImaGene version 9.0 software (BioDiscovery). The quantified signals were background-corrected (Normexp with offset value 10 (32)) and normalized using quantile normalization.

Western Blotting—Proteins were harvested from cells as described previously (29). Cell lysates (10–20 μg) were fractionated by SDS-PAGE and electrophoretically transferred to nitrocellulose membranes. Membranes were blocked in nonfat dry milk (5%) and incubated overnight with primary antibody against TTF-1 (clone 8G7G3/1, Santa Cruz Biotechnology, Inc. (Santa Cruz, CA)), HMGA2 (Biocheck), GAPDH (Cell Signaling), or HSP90 (BD Transduction Laboratories). Proteins were detected with appropriate HRP-conjugated secondary antibody (Thermo Scientific) and chemiluminescent substrates.

TABLE 1
List of PCR primers used in this study

Name	Direction	Sequence
Mouse RT-QPCR primers		
Gapdh	Forward	5′-GCTTGTCATCAACGGGAAGC-3′
	Reverse	5′-TTTGATGTTAGTGGGGTCTCGC-3′
Ttf-1	Forward	5′-AAAACTGCGGGGATCTGAG-3′
	Reverse	5′-TGCTTTGGACTCATCGACAT-3′
Srebf1	Forward	5′-CCAGAGGGTGAGCCTGACA-3′
	Reverse	5′-AGCCTCTGCAATTTCCAGATCT-3′
Srebf2	Forward	5′-TGTGAACCTGGCCGAGTGT-3′
	Reverse	5′-CGCTGTCAGGTGGATCTCAA-3′
Hmga2	Forward	5′-GGGCGCCGACATTCAAT-3′
	Reverse	5′-ACTGCAGTGTCTTCTCCCTTCAA-3′
Human RT-QPCR primers		
GAPDH	Forward	5′-GGAGTCAACGGATTTGGTCGTA-3′
	Reverse	5′-GGCAACAATATCCACTTTACCAGAGT-3′
TTF1	Forward	5′-CGTTCTCAGTGTCTGACATCTTGA-3′
	Reverse	5′-CCTCCATGCCCACTTTCTTG-3′
SREBF1	Forward	5′-GCTCCTCCATCAATGACAAAATC-3′
	Reverse	5′-TGCAGAAAGCGAATGTAGTCGA-3′
SREBF2	Forward	5′-CGAATTGAAAGACCTGGTCATG-3′
	Reverse	5′-TCCTCAGAACGCCAGACTTGT-3′
HMGA2	Forward	5′-CCCAAAGGCAGCAAAAACAA-3′
	Reverse	5′-GCCTCTTGGCCGTTTTTCTC-3′
ChIP QPCR primers		
C9Orf5 (distal)	Forward	5′-TGTCTGCCTTAAAAGCTTGTGTTC-3′
	Reverse	5′-TTTGCTCCAGTACTTTGCACACTT-3′
C9Orf5 (proximal)	Forward	5′-GGTATTCTAGTATGCAGCTTGGGTTT-3′
	Reverse	5′-GAAGCTCCTTTCACTCATTCGTTAA-3′
SREBF2 (distal)	Forward	5′-GAAGCGTGAATTGGCCTTATG-3′
	Reverse	5′-TCTGACCCTTTCCCGTTGAT-3′
SREBF2 (proximal)	Forward	5′-GCAAAGCAGAAGACGTAAAATCC-3′
	Reverse	5′-CACGGAGGCTTGACAAGGTT-3′
SPB (distal)	Forward	5′-CCGAAGGCTGTAGGGAAGAA-3′
	Reverse	5′-GCTCAGGAACACTAGGGATTGC-3′
SPB (proximal)	Forward	5′-TCCACCCACAAAAGCACTGTAG-3′
	Reverse	5′-TCTCCCTAGTGGAGGCTCACA-3′
HMGA2 3′-UTR psiCHECK2 site-directed mutagenesis primers[a]		
Δ1	Forward	5′-CAGGGGACACAGCTTAAGGTACCCTTTTAATTACTG-3′
	Reverse	5′-CAGTAATTAAAAGGGTACCTTAAGCTGTGTCCCCTG-3′
Δ2	Forward	5′-GCTGCTATACACAAGGGTACCGAAAAAAACTTACTG-3′
	Reverse	5′-CAGTAAGTTTTTTTCGGTACCCTTGTGTATAGCAGC-3′
Δ3	Forward	5′-GCCCTGCTTTTGCATGGTACCTCAAAAATATGTG-3′
	Reverse	5′-CACATATTTTTGAGGTACCATGCAAAAGCAGGGC-3′

[a] The KpnI cut site is underlined.

Luciferase Reporter Assays—Promoter reporter assays were carried out in 96-well plates as described previously (29). Briefly, cells were co-transfected with a firefly luciferase reporter construct and a *Renilla* luciferase control vector pGL4.73 (Promega). Twenty-four hours after transfection, firefly and *Renilla* luciferase values were quantified using Dual-Glo luciferase assay (Promega) on a GloMax-96 plate reader (Promega). Firefly luciferase values were normalized to *Renilla* luciferase values and expressed as relative values. For 3′-UTR-based reporter studies, cells were seeded onto 24-well plates and co-transfected with psiCHECK2 reporter constructs (300 ng) and RNA oligonucleotides on the following day. Firefly and *Renilla* luciferase values were measured 48 h after transfection, and *Renilla* luciferase signals were normalized to firefly luciferase signals.

Chromatin Immunoprecipitation (ChIP)—ChIP was performed on NCI-H441 cells as described previously (29), using either a TTF-1 antibody (H190) or a normal rabbit IgG (Santa Cruz Biotechnology, Inc.). Target sequences were detected by QPCR using Brilliant II SYBR Green master mix (Stratagene). QPCR signals of the immunoprecipitated chromatins were normalized to the signal from the total lysate (input) for each primer pair. Primers used for ChIP analyses are listed in Table 1.

Transwell Migration and Invasion Assays—For Boyden chamber migration assays, 5×10^4 transfected cells were seeded in triplicate onto upper chamber of a migration insert with 8-μm pore size (catalog no. 354578, BD Biosciences) in serum-free media; media supplemented with 5% fetal bovine serum, as a chemoattractant, was added to the lower well. After 24 h, cells from the top of the chamber membrane were removed, and the remaining cells on the bottom of the membrane were fixed with methanol and stained with hematoxylin. Average nuclei were determined in five ×100 fields using a Nikon Eclipse microscope and NIS Elements D software (Nikon), with nuclei counted blind and manually. Invasion assays were performed in the same manner as the migration assay but utilized Matrigel-coated inserts with 8-μm pore size (catalog no. 354480, BD Biosciences).

Statistical Analysis—GraphPad Prism version 5 software was used to perform statistical analyses, including Student's *t* test, when comparing two groups (control and experimental). One-way analysis of variance with Tukey's post-test was used to compare more than two groups, and a two-way analysis of vari-

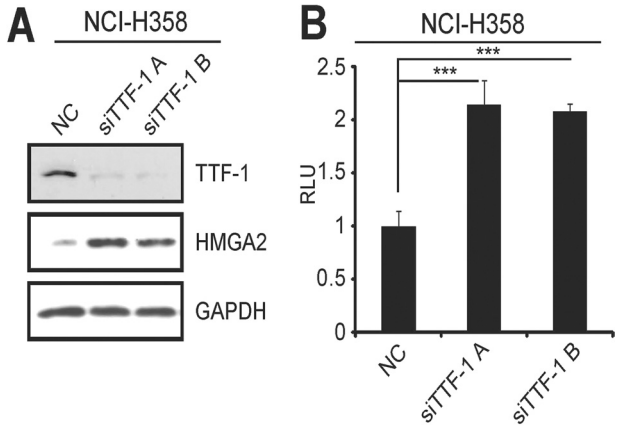

FIGURE 1. **TTF-1 negatively regulates HMGA2 in NCI-H358 cells.** *A*, NCI-H358 cells were transfected with non-targeting RNA oligonucleotide (negative control; *NC*) or two separate siRNAs targeting TTF-1 (siTTF-1 A and B), and proteins were harvested after 72 h. Protein levels of TTF-1, HMGA2, and GAPDH (loading control) were determined by immunoblotting. *B*, NCI-H358 cells were transfected with a negative control or siTTF-1-targeting siRNAs, along with a psiCHECK2 vector containing the *HMGA2* 3′-UTR fused to the 3′-end of a *Renilla* luciferase gene. Luciferase assays were performed after 48 h ($n = 3$). *RLU*, relative luminescence units. *Error bars*, S.D. ***, $p < 0.001$.

ance test was used to analyze time course experiments. Representative experiments repeated at least twice are shown as mean ± S.D. Data were considered statistically significant when p was <0.05 (*, $p < 0.05$; **, $p < 0.01$; ***, $p < 0.001$).

RESULTS

TTF-1 Represses HMGA2 in Human Lung Cancer Cells—Winslow *et al.* (24) reported a surprising finding, that *Ttf-1* suppresses metastasis formation of primary lung adenocarcinomas driven by mutant *Kras* and *p53* loss ($Kras^{G12D/+}$;$p53^{\Delta/\Delta}$) in a mouse model system. By gene expression profiling and functional analyses, it was determined that a pro-EMT oncogene, *Hmga2*, is a downstream target of Ttf-1 and that repression of *Hmga2* expression by Ttf-1 is a basis to the antimetastatic activity of *Ttf-1* (24). To test if the Ttf-1/Hmga2 relationship is conserved in human lung cancer cells, we used two independent small interfering RNAs (siRNAs) against *TTF-1* to knock down the endogenous expression of TTF-1 in a human lung adenocarcinoma cell line with endogenous HMGA2 protein expression (NCI-H358). Interestingly, both siTTF-1s led to a greater than 2-fold derepression in HMGA2 protein expression (Fig. 1*A*). This observation suggests that the Ttf-1 ⊣ Hmga2 axis, originally discovered in the murine lung adenocarcinoma cells derived from tumors initiated by somatic activation of oncogenic Kras and p53 deletion (24), holds true in human lung cancer cells as well.

Although it is known that *HMGA2* is subject to regulation by the let-7 family of miRNAs (33), let-7s do not appear to play a role in mediating the repression of Hmga2 by Ttf-1 in murine lung cancer cells (24). Thus, we hypothesized that there are other miRNAs mediating the Ttf-1/Hmga2 regulation. To this end, we utilized a reporter plasmid where the 3′-UTR of human *HMGA2* was fused to the 3′-end of the *Renilla* luciferase gene in the psiCHECK2 vector backbone (30). This reporter plasmid was transfected into the NCI-H358 human lung cancer cell line in which the endogenous TTF-1 expression was knocked down using two independent siTTF-1s. The results demonstrate that a decrease of TTF-1 expression leads to a concomitant increase in the luciferase activity of Luc-HMGA2/3′-UTR (Fig. 1*B*). This derepression of *HMGA2* 3′-UTR upon TTF-1 knockdown implicates the involvement of *HMGA2* 3′-UTR in the TTF-1-induced silencing of *HMGA2*.

Discovery of miRNAs That Mediate the Ttf-1 ⊣ Hmga2 Relationship in Murine Lung Cancer Cells—Our working hypothesis was that TTF-1 may directly up-regulate certain miRNAs, which in turn repress *HMGA2* expression via direct binding to the 3′-UTR of *HMGA2*. To identify these putative miRNA regulators, we utilized the non-metastatic (TnonMet) murine primary lung tumor cells (394T4) generated and modified by Winslow *et al.* (24) to stably express a small hairpin RNA (shRNA) against *Ttf-1* (394T4-shTtf-1). The *Ttf-1* knockdown and the corresponding *Hmga2* up-regulation in 394T4-shTtf-1 cells elicited a higher metastatic phenotype, whereas the control cells, 394T4-shLuc carrying an shRNA against luciferase (shLuc), were non-metastatic and thus similar to the parental 394T4 cells (24). We reasoned that the putative miRNA(s) responsible for suppressing *Hmga2* in a Ttf-1-dependent manner in the 394T4-shLuc ($Ttf\text{-}1^{high}$) cells would be down-regulated in 394T4-shTtf-1 ($Ttf\text{-}1^{low}$) cells due to Ttf-1 knockdown. To identify these miRNA regulators that are present in both mice and humans, we created a custom QPCR array that contains 44 LNA-based QPCR probes in duplicates (Exiqon). Each of the LNA probes detects an miRNA predicted by TargetScan version 5.2 (34) to bind to human *HMGA2* 3′-UTR (Table 2). Approximately 57% (*i.e.* 25) of the 44 human miRNA probes are able to detect the mouse counterparts based on sequence conservation. This QPCR array was employed to quantify the murine miRNA expression differences between 394T4-shLuc ($Ttf\text{-}1^{high}$) and 394T4-shTtf-1 ($Ttf\text{-}1^{low}$) cells. Twelve murine miRNAs were scored in the QPCR array assay, and the results are presented as ratios of miRNA expression levels (shLuc/shTtf-1; Fig. 2*A*). Interestingly, two human miRNA probes (hsa-miR-33a and hsa-miR-495) detected high expression ratios, suggesting that the two corresponding murine miRNAs may be positively regulated by Ttf-1. Indeed, secondary confirmational studies utilizing an independent miRNA detection system (Quanta Biosciences) validated the QPCR array data for mmu-miR-33 (*i.e. Ttf-1* knockdown repressing mmu-miR-33 expression) (Fig. 2*B*). (Note that mmu-miR-33 is the mouse homolog of human hsa-miR-33a. The two miRNAs are 100% identical in sequence. Hereafter, hsa-miR-33a and mmu-miR-33 are referred to as miR-33a and miR-33, respectively.) We did not pursue the second positive hit of the QPCR array screen (mmu-miR-495) because this miRNA, unlike miR-33, was not predicted to target the mouse *Hmga2* 3′-UTR by TargetScan; therefore, mmu-miR-495 is not likely to be involved in the Ttf-1-mediated repression of *Hmga2* in the murine lung cancer cells.

Searching for TTF-1-regulated miRNAs in a Human Lung Epithelial System with Inducible TTF-1 Expression—To substantiate the candidacy of miR-33a as a TTF-1-regulated miRNA and to explore TTF-1-regulated miRNAs globally in human cells, we took on a gain-of-function strategy using a human lung epithelial cell system in which the expression of a

TABLE 2
Probe list of the custom *HMGA2*-3′-UTR-targeting QPCR array

	miRNA	Comment
1	hsa-let-7b	Included in analysis
2	hsa-let-7c	Included in analysis
3	hsa-let-7d	Included in analysis
4	hsa-let-7e	Included in analysis
5	hsa-let-7f	Included in analysis
6	hsa-let-7i	Included in analysis
7	hsa-miR-186	Included in analysis
8	hsa-miR-26b	Included in analysis
9	hsa-miR-33a	Included in analysis
10	hsa-miR-495	Included in analysis
11	hsa-miR-532-3p	Included in analysis
12	hsa-miR-9	Included in analysis
13	hsa-miR-137	Not detected
14	hsa-miR-196a	Not detected
15	hsa-miR-204	Not detected
16	hsa-miR-361-5p	Not detected
17	hsa-miR-370	Not detected
18	hsa-miR-539	Not detected
19	hsa-let-7a	Excluded, replicate *Ct* >1.5 cycles
20	hsa-let-7g	Excluded, replicate *Ct* >1.5 cycles
21	hsa-miR-129-5p	Excluded, replicate *Ct* >1.5 cycles
22	hsa-miR-196b	Excluded, replicate *Ct* >1.5 cycles
23	hsa-miR-26a	Excluded, replicate *Ct* >1.5 cycles
24	hsa-miR-760	Excluded, replicate *Ct* >1.5 cycles
25	hsa-miR-98	Excluded, replicate *Ct* >1.5 cycles
26	hsa-miR-202	Excluded, human-specific miRNA
27	hsa-miR-211	Excluded, human-specific miRNA
28	hsa-miR-337-3p	Excluded, human-specific miRNA
29	hsa-miR-33b	Excluded, human-specific miRNA
30	hsa-miR-376c	Excluded, human-specific miRNA
31	hsa-miR-450b-5p	Excluded, human-specific miRNA
32	hsa-miR-509-3-5p	Excluded, human-specific miRNA
33	hsa-miR-520d-5p	Excluded, human-specific miRNA
34	hsa-miR-522	Excluded, human-specific miRNA
35	hsa-miR-524-5p	Excluded, human-specific miRNA
36	hsa-miR-548c-3p	Excluded, human-specific miRNA
37	hsa-miR-554	Excluded, human-specific miRNA
38	hsa-miR-556-5p	Excluded, human-specific miRNA
39	hsa-miR-570	Excluded, human-specific miRNA
40	hsa-miR-573	Excluded, human-specific miRNA
41	hsa-miR-578	Excluded, human-specific miRNA
42	hsa-miR-579	Excluded, human-specific miRNA
43	hsa-miR-588	Excluded, human-specific miRNA
44	hsa-miR-608	Excluded, human-specific miRNA

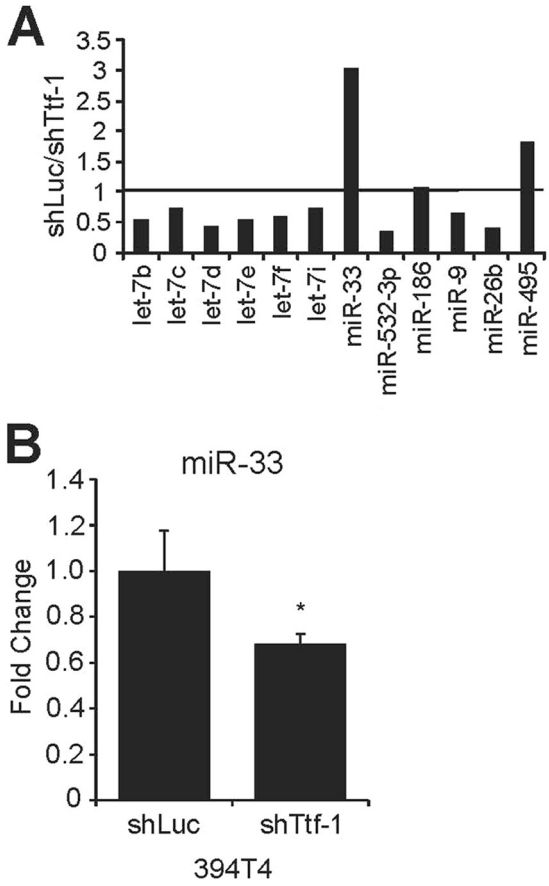

FIGURE 2. **Screening murine lung cancer cells for Ttf-1-regulated miRNAs that target HMGA2 using an LNA-QPCR array.** *A*, total RNA isolated from 394T4-shLuc (Ttf-1^{high}) and 394T4-shTtf-1 (Ttf-1^{low}) cells was quantified in duplicate using an LNA-QPCR array designed to include miRNAs predicted to target the 3′-UTR of human *HMGA2* gene. Normalized expression values between the two cell lines are expressed as -fold change of shLuc over shTtf-1 cells. *B*, down-regulation of mmu-miR-33 in 394T4-shTtf-1 cells was confirmed by RT-QPCR using an miRNA detection system and PCR primers (Quanta Biosciences) ($n = 3$). *Error bars*, S.D. *, $p < 0.05$.

human *TTF-1* transgene could be turned on by doxycycline (*i.e.* a doxycycline (dox)-on system) (29). The host cells of this inducible system are the premalignant, viral oncogene-immortalized human lung epithelial cells, BEAS-2B (35). We chose this cell strain due to the fact that it lacks endogenous TTF-1 expression (36), thus maximizing the miRNA expression perturbation in response to the dox-induced expression of the *TTF-1* transgene. As shown by immunoblotting, the expression of TTF-1 protein was turned on following a 24-h dox treatment (Fig. 3*A*), with little leaky expression of the *TTF-1* transgene without dox in the culture media. Concomitantly, *HMGA2* mRNA decreased by 40% upon dox induction (data not shown). For global miRNA profiling, we collected total RNA from these four samples in duplicates: (i) BEAS-2B-rtTA3-TTF-1 in the presence of dox (TTF-1 + Dox), (ii) BEAS-2B-rtTA3-TTF-1 in the absence of dox (TTF-1 − Dox), (iii) BEAS-2B-rtTA3-empty vector in the presence of dox (EV + Dox), and (iv) BEAS-2B-rtTA3-empty vector in the absence of dox (EV − Dox). The *TTF-1* transgene was turned on only under the (i) TTF-1 + Dox condition. These RNAs were analyzed for global miRNA expression using a commercial microarray platform (Exiqon miRCURY^{TM} LNA microRNA Array 5th Generation; the number of miRNA species the array targeted was as follows: 1250 human, 1115 mouse, and 692 rat). Two outliers, hsa-miR-33a and hsa-miR-32, were up-regulated in the TTF-1 + Dox group relative to either the TTF-1 − Dox or EV + Dox group (Fig. 3*B*; see supplemental Table S1 for the complete list of differentially expressed miRNAs), suggesting that the observed expression

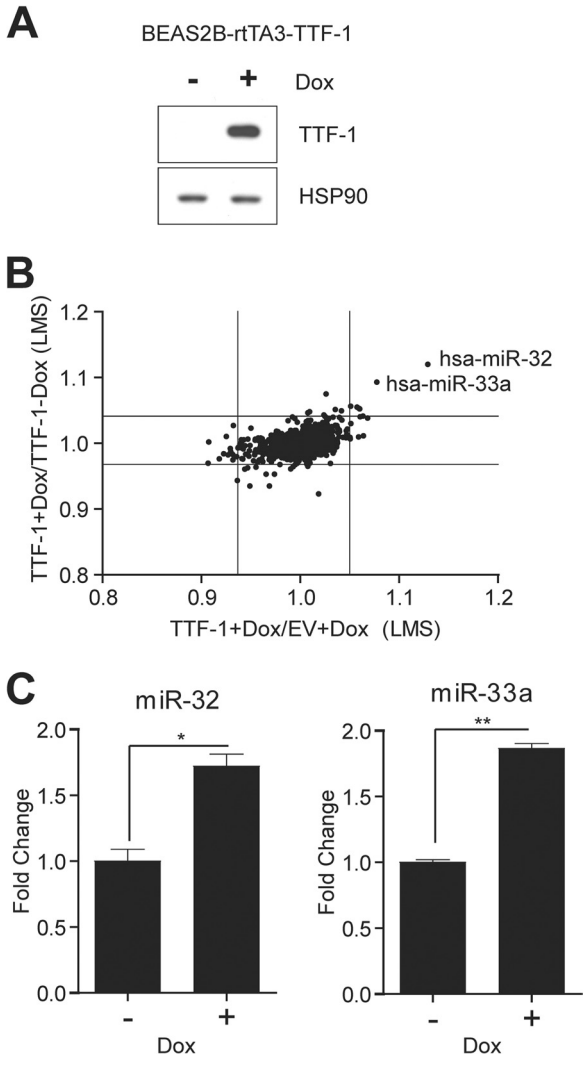

FIGURE 3. **A global screen for TTF-1-regulated miRNAs using a microarray platform.** *A*, immortalized human lung epithelial cells with Dox-inducible TTF-1 elements (BEAS-2B-rtTA3-TTF1) were treated with or without dox (0.8 μg/ml) for 24 h prior to protein harvest. Western blot analysis confirmed the induction of TTF-1, with HSP90 protein as the loading control. *B*, RNA isolated from BEAS-2B-rtTA3-EV or TTF-1 cells treated with or without dox (0.8 μg/ml) for 24 h was evaluated in duplicates for changes in miRNA expression using an LNA-miRNA microarray (Exiqon). Expression of miRNAs between the different groups was compared by log median scores (*LMS*), and the average miRNA expression changes are graphed as indicated. *Lines* on the graph indicate the 1st and 99th percentile of the data. *C*, up-regulation of miR-32 and miR-33a in BEAS-2B-rtTA3-TTF-1 cells was confirmed using RT-QPCR ($n = 3$). *Error bars*, S.D. *, $p < 0.05$; **, $p < 0.01$.

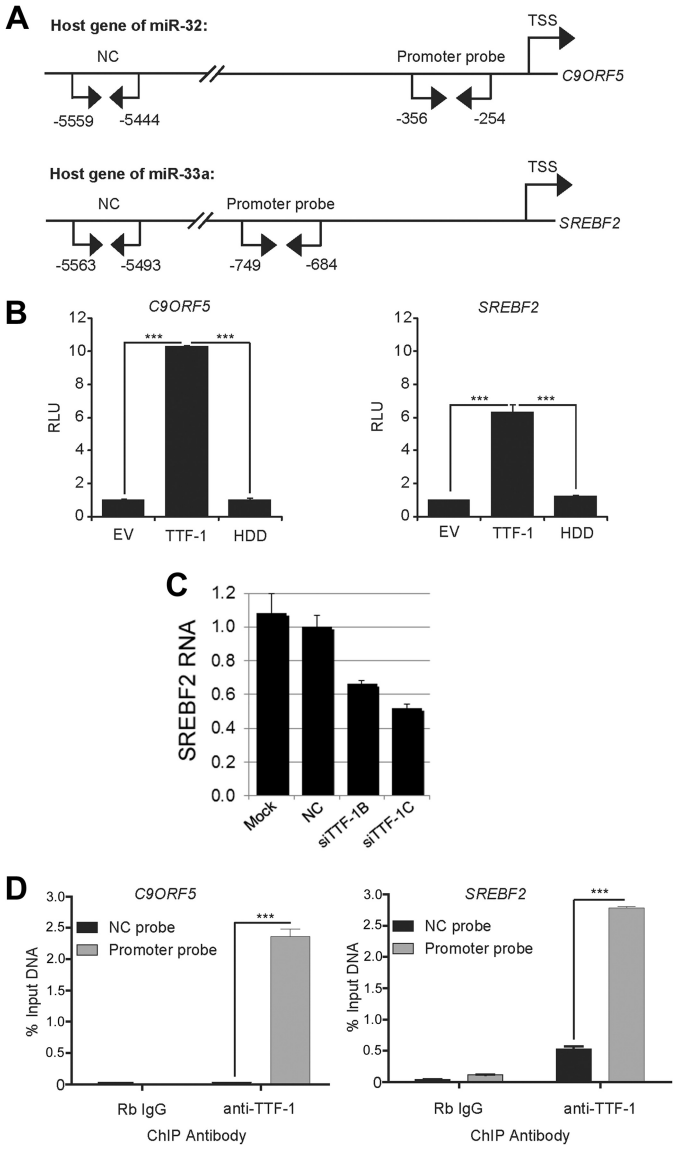

FIGURE 4. **TTF-1 binds to and activates transcription from the promoters of the miR-32 and miR-33a host genes.** *A*, diagram of the promoter regions of the miR-32 and miR-33a host genes, *C9Orf5* and *SREBF2*, respectively. Locations for negative control (*NC*) and promoter PCR primer pairs used in the ChIP analyses are shown relative to the respective gene's predicted transcriptional start site (*TSS*). *B*, A549 cells were transfected with the indicated expression vector (empty vector (*EV*), TTF-1, or a TTF-1 homeodomain deletion mutant, *HDD*) and a luciferase promoter reporter construct for *C9Orf5* (miR-32) or *SREBF2* (miR-33a). Luciferase assays were performed 24 h after transfection ($n = 4$). *y axis*, -fold change in relative luminescence units (*RLU*). *C*, *TTF-1* knockdown resulted in a decrease of *SREBF2* RNA. NCI-H441 cells were transfected with mock or a negative control oligonucleotide or an individual siTTF-1. After 48 h, RT-QPCR was conducted to quantify the expression level of *SREBF2* RNA ($n = 3$). SiTTF-1B and SiTTF-1C were from Dharmacon/Thermo Scientific (catalog nos. D019105-04 and D019105-17, respectively). *D*, chromatin immunoprecipitation of endogenous TTF-1 in NCI-H441 cells. Sheared chromatins were precipitated with either rabbit immunoglobulin (Rb IgG) or anti-TTF-1 antibody and subsequently analyzed using QPCR location probes shown in *A* ($n = 3$). *Error bars*, S.D. ***, $p < 0.001$.

changes were dependent on TTF-1 expression but independent of dox treatment. For validation, LNA-based probes to miR-33a and miR-32 were used in RT-QPCR to confirm the array profiling data. The results, corroborating the array profiling observations, indicate a 1.7–2-fold increase of miR-33a and miR-32 upon TTF-1 induction (Fig. 3*C*).

Identification of miR-33a and miR-32 as Direct Transcriptional Targets of TTF-1—In view of the biochemical property of TTF-1 as a transcription factor (17, 37, 38), we surmised that TTF-1 would activate the promoter of the respective genes hosting miR-33a and miR-32. To approach this issue, we cloned the promoter region (~1 kb) of *SREBF2* (NM_004599, the host gene of hsa-miR-33a) and *C9ORF5* (NM_032012, the host gene of hsa-miR-32) into the 5′-end of a promoterless luciferase reporter vector (Fig. 4*A*). The luciferase activity readout of the resultant reporter plasmids was then used to assess the responsiveness of each promoter to TTF-1 or a transcriptionally inactive mutant of TTF-1 lacking the homeodomain (the homeodomain deletion mutant (29)) in A549 cells, a human lung cancer

TABLE 3
Top five predicted targets for hsa-miR-33a and mmu-miR-33 by TargetScan 5.2 and 6.2

Rank	Target gene	Gene name	Total context score
hsa-miR-33a TargetScan 5.2			
1	*ABCA1*	ATP-binding cassette, subfamilyA (ABC1), member 1	−1.25
2	*CROT*	Carnitine *O*-octanoyltransferase	−0.84
3	*CDK6*	Cyclin-dependent kinase 6	−0.8
4	*HMGA2*	High mobility group AT-hook 2	−0.75
5	*LIMCH1*	LIM and calponin homology domains 1	−0.71
mmu-miR-33 TargetScan 5.2			
1	*Abca1*	ATP-binding cassette, subfamilyA (ABC1), member 1	−0.86
2	*Hmga2*	High mobility group AT-hook 2	−0.83
3	*Slc12a5*	Solute carrier family 12, member 5	−0.74
4	*Zfp281*	Zinc finger protein 281	−0.72
5	*Rgs7bp*	Regulator of G-protein signaling 7-binding protein	−0.67
hsa-miR-33a TargetScan 6.2			
1	*ABCA1*	ATP-binding cassette, subfamilyA (ABC1), member 1	−0.88
2	*CROT*	Carnitine *O*-octanoyltransferase	−0.65
3	*CCNYL1*	Cyclin Y-like 1	−0.54
4	*PCDH18*	Protocadherin 18	−0.5
5	*AKAP2*	A kinase (PRKA) anchor protein 2	−0.48
32	*HMGA2*	High mobility group AT-hook 2	−0.36
mmu-miR-33 TargetScan 6.2			
1	*Abca1*	ATP-binding cassette, subfamilyA (ABC1), member 1	−0.72
2	*Slc12aA5*	Solute carrier family 12 (potassium/chloride transporter), member 5	−0.65
3	*Hmga2*	High mobility group AT-hook 2	−0.52
4	*Znf281*	Zinc finger protein 281	−0.52
5	*Dcun1d5*	DCN1, defective in cullin neddylation 1, domain-containing 5	−0.47

cell line commonly used to study transcriptional activity of exogenous TTF-1 (39). The data in Fig. 4*B* show that both promoters respond to TTF-1 transactivation, whereas the homeodomain deletion mutant of TTF-1 failed to activate the promoters, consistent with the notion that the homeodomain-dependent DNA binding activity of TTF-1 is essential for this function (40). The positive luciferase data are in line with the thesis that *SREBF2* is under TTF-1 transcriptional control. To further test this relationship, we used two siTTF-1s to knock down endogenous TTF-1 in the NCI-H441 human lung adenocarcinoma cell line, which has high endogenous TTF-1 expression (29). RT-QPCR analyses show that TTF-1 knockdown induced a concomitant 40–50% decrease in *SREBF2* RNA (Fig. 4*C*).

To determine whether TTF-1 directly bound to the promoters of the respective host genes of miR-33a and miR-32, we conducted ChIP using an anti-TTF-1 antibody. The immunoprecipitated chromatins from NCI-H441 cells were analyzed using two genomic location probes: a proximal probe at <1 kb and a distal probe at 5 kb upstream to the transcription start site (Fig. 4*A*, *TSS*). In both cases, the proximal QPCR probes detected quantitative recovery of promoter DNA sequences for both host genes in the TTF-1-precipitated chromatins immunoprecipitated (Fig. 4*D*), implying a direct interaction between the promoter region of both host genes with TTF-1. In view of the positive results for miR-33a in both loss- and gain-of-function analyses using mouse and human cells, miR-33a stood out as a strong candidate miRNA under direct TTF-1 control.

TTF-1-induced Down-regulation of HMGA2 Is Mediated by miR-33a—Both human *HMGA2* and mouse *Hmga2* were ranked by TargetScan (34) as potential target genes of hsa-miR-33a and mmu-miR-33, respectively (Table 3). In addition, there are three putative binding sites for miR-33a and one binding site for miR-32 in the *HMGA2* 3′-UTR (Fig. 5*A*). In view of these data, we initiated studies to validate *HMGA2* as an authentic target gene of miR-33a and miR-32. An miR-33a mimetic oligonucleotide or an miRNA known to target *HMGA2* (let-7d) was cotransfected with a luciferase reporter of *HMGA2* 3′-UTR into a human lung cancer cell line, NCI-H1299. We chose NCI-H1299 because the endogenous HMGA2 expression in NCI-H1299 is responsive to let-7 regulation (13), implicating the existence of a functional miRNA-dependent surveillance of *HMGA2* in NCI-H1299 cells. Chemiluminescence measurement revealed a 50% reduction of reporter activity in the miR-33a transfectants (Fig. 5*B*); the positive control let-7d induced a stronger inhibition of *HMGA2* 3′-UTR reporter (~80%), which is probably due to the fact that there are seven let-7 binding sites in the 3′-UTR of *HMGA2* (Fig. 5*A*). Interestingly, although the miR-32 mimic elicited a slight response in the reporter assay, this response appeared to be independent of the predicted miR-32 site (Fig. 5*C*). Thus, we conclude that the predicted binding site of miR-32 in the 3′-UTR of *HMGA2* may be nonfunctional. We then proceeded to measure the endogenous RNA and protein expression of *HMGA2* following miR-33a or let-7d transfection in NCI-H1299 cells (Fig. 5, *D* and *E*). In addition, we also measured the HMGA2 protein level following miR-33a transfection in the murine lung cancer cells (394T4-shTtf-1; Fig. 5*F*). Overall the results corroborate the notion that *HMGA2* is a target gene of miR-33a.

To substantiate that the Ttf-1-induced up-regulation of mmu-miR-33 in the 394T4 murine cells was responsible for repressing *Hmga2*, we first treated 394T4-shLuc (Ttf-1^{high}) cells with an miR-33a miRNA inhibitor (anti-miR-33a, which targets both hsa-miR-33a and mmu-miR-33) and found that the Hmga2 protein level increased by ~2-fold (Fig. 6*A*). To extend this observation to human lung cancer cells, we next treated NCI-H358 cells with anti-miR-33a. Inhibition of miR-

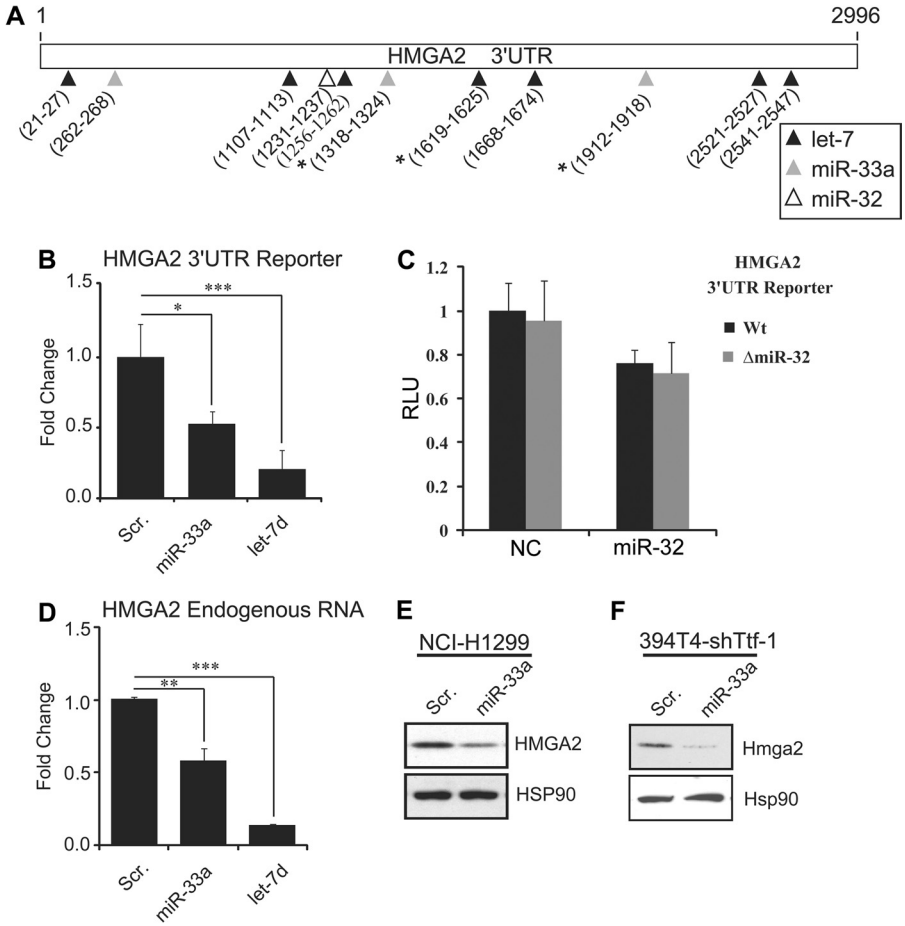

FIGURE 5. **HMGA2 is a novel target of miR-33a in mouse and human lung cancer cells.** *A*, diagram depicting the 3′-UTR of the human *HMGA2* gene. Locations of predicted miRNA binding sites for let-7 (*black*), miR-33a (*gray*), and miR-32 (*white*) are marked with *arrows*, and seed site locations are listed *below* the *arrows*. *B*, NCI-H1299 cells were transfected with the *HMGA2* 3′-UTR reporter and either a scrambled control oligonucleotide (*Scr*) or an miR-33a mimic (*miR-33a*). Luciferase activity was read 48 h post-transfection ($n = 3$). *C*, *HMGA2* 3′-UTR is not a target for miR-32. NCI-H1299 cells were cotransfected with an miR-32 mimic or a negative control oligonucleotide (*NC*). At the same time, the transfections include a wild-type *HMGA2* 3′-UTR reporter construct (*Wt*) or an *HMGA2* 3′-UTR reporter with a deleted miR-32 binding site (Δ*miR-32*). After 48 h, *Renilla* and firefly luciferase activities were assayed. Although miR-32 resulted in a slight inhibition of the *HMGA2* reporter, deletion of the sole predicted miR-32 binding site did not cause a derepression of the *HMGA2* reporter. *RLU*, relative luminescence units. *D*, quantification of endogenous *HMGA2* mRNA after transfection of NCI-H1299 cells with a scrambled control oligonucleotide or an miR-33a mimic. *HGMA2* expression levels were normalized to GAPDH ($n = 3$). *E*, Western blot analysis confirmed a reduced expression of HMGA2 in the human NCI-H1299 cells transfected with miR-33a mimic. *F*, the Hmga2 expression was knocked down in the murine 394T4-shTtf-1 cells transfected with an miR-33a mimic. *, $p < 0.05$; **, $p < 0.01$; ***, $p < 0.001$.

33a in these cells again resulted in a ~3-fold increase in HMGA2 protein (Fig. 6*B*), corroborating the results seen with the murine 394T4-shLuc cells. Finally, we analyzed the impact of anti-miR-33a on the Hmga2 repression imposed by exogenous TTF-1. To this end, we transfected human *TTF-1* cDNA into a murine *Ttf-1* knockdown background (394T4-shTtf-1 cells). The stably expressed shRNA against the mouse *Ttf-1* gene in the 394T4-shTtf-1 cells does not down-regulate the human *TTF-1* gene due to the fact the particular shRNA targeting sequence (CGCCATGTCTTGTTCTACCTT) is unique to mouse *Ttf-1*. The expression of human TTF-1 clearly conferred repression of Hmga2 (Fig. 6*C*). Importantly, anti-miR-33a abolished the Hmga2 protein repression imposed by the exogenous human TTF-1 (Fig. 6*C*), proving that miR-33a is a critical mediator of the TTF-1-induced *HMGA2* repression.

Analysis of miR-33a Binding Sites in the 3′-UTR of HMGA2—To analyze the relative contribution of the three miR-33a binding sites to *HMGA2* repression by miR-33a, we mutated the three TargetScan-predicted miR-33a binding sites individually

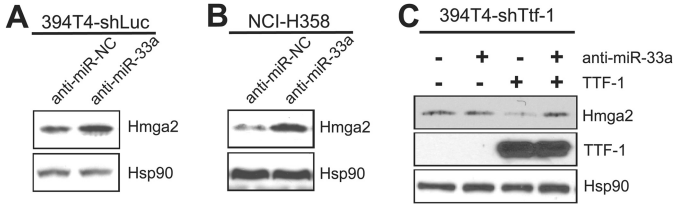

FIGURE 6. **TTF-1 up-regulation of miR-33a suppresses HMGA2 expression in human and mouse lung epithelial cells.** *A*, Western blot analysis of Hmga2, Ttf-1, and Hsp90 expression in murine 394T4-shLuc cells transfected with either a negative control (*anti-miR-NC*) or an miR-33a inhibitor (*anti-miR-33a*). *B*, Western blot analysis of HMGA2, TTF-1, and Hsp90 expression in the human NCI-H358 cells transfected with either a negative control or an miR-33a inhibitor. *C*, 394T4-shTtf-1 cells were transfected as indicated, and the corresponding cell lysates were analyzed by immunoblotting for the expression of Ttf-1, Hmga2, and Hsp90.

and in all possible pairwise combinations, affording a total of seven mutant reporter plasmids of *HMGA2* 3′-UTR for analysis (Fig. 7*A*). The luciferase reporter activities of individual mutant plasmids were evaluated following cotransfection into NCI-H1299 cells along with either an exogenous miR-33a mimetic

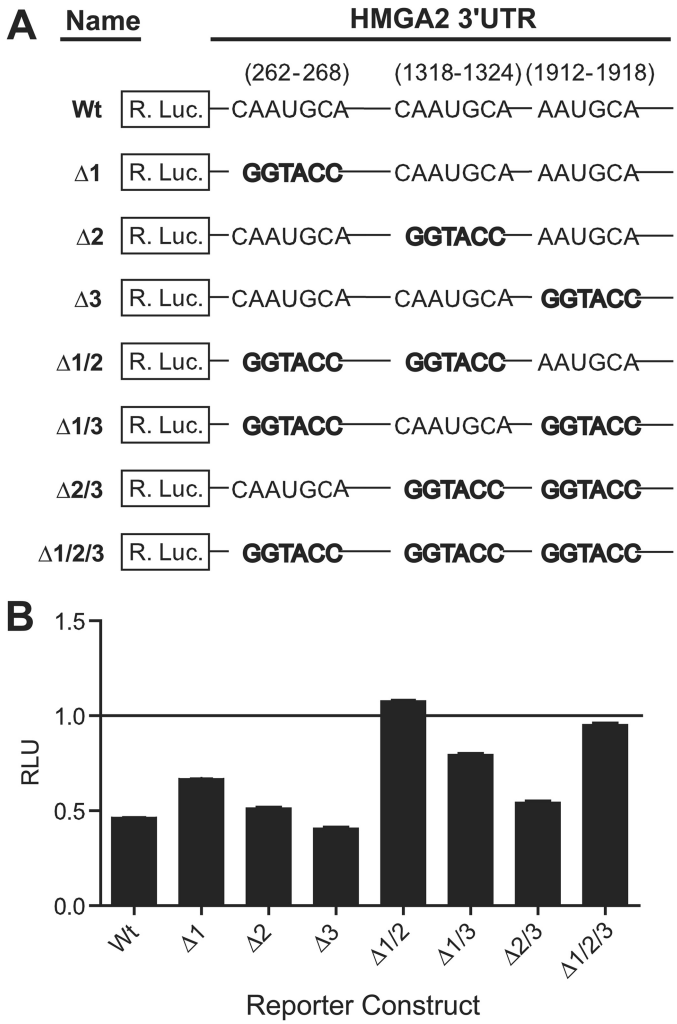

FIGURE 7. **Characterization of the three predicted miR-33a binding sites located within the HMGA2 3′-UTR.** *A*, diagram depicting the *HMGA2* 3′-UTR reporter construct mutants used to characterize functional miR-33a sites. The miR-33a seed sequences were mutated by replacement with a KpnI restriction enzyme recognition sequence (GGTACC). *B*, NCI-H1299 cells, transfected with individual *HMGA2* 3′-UTR reporter constructs from *A* and an miR-33a mimetic oligonucleotide or a scrambled control oligonucleotide (each at 20 nM), were assayed for luciferase activities 48 h post-transfection. Relative luminescence units (*RLU*) were normalized to the corresponding scrambled control for each reporter construct ($n = 3$). *Error bars*, S.D.

oligonucleotide or a scrambled control oligonucleotide. Of the three single-site mutants (Δ1, Δ2, and Δ3), Δ1 showed the strongest derepression (Fig. 7*B*), whereas Δ3 was essentially identical to the wild-type reporter plasmid. This suggests that the relative contribution of the three miR-33a binding sites to repression of *HMGA2* 3′UTR is in the following order: site 1 > site 2 > site 3. Data obtained with the three double mutants (Δ1/2, Δ1/3, and Δ2/3) generally agreed with the observation gathered from single mutants (Fig. 7*B*). It is intriguing to note that the derepression of losing both sites 1 and 2 (Δ1/2) appeared to be larger than the sum of the two single mutants (Δ1 + Δ2), indicating potential synergy between sites 1 and 2. Although miRNA binding sites are known to work synergistically in repressing target genes, the two miRNA binding sites would generally have to be close in distance for optimal cooperativity (34, 41). Therefore, in view of the long distance (>1 kb) between miR-33a sites 1 and 2 in the 3′-UTR of *HMGA2*, it is surprising that these two sites might work cooperatively.

miR-33a Impedes Motility of Human and Murine Lung Cancer Cells—Because Ttf-1 was shown to regulate metastatic dissemination (24), we chose to examine the migratory and invasive properties of human and murine lung cancer cells following modulation of TTF-1/miR-33a/HMGA2 levels. Initially, we compared the migration and invasiveness of the two murine lung cancer cell lines, 394T4-shLuc (Ttf-1^{high}) and 394T4-shTtf-1 (Ttf-1^{low}), using transwell migration (uncoated control inserts) and invasion (Matrigel-coated inserts) assays. Although the motility of the 394T4-shTtf-1 cells was greater than the shLuc cells, there was no difference in invasiveness between the treatment groups (Fig. 8, *A* and *B*). Transfection of the human NCI-H1299 cells with an exogenous miR-33a oligonucleotide impeded migration compared with a scrambled control oligonucleotide in the transwell migration assay. However, the invasiveness of cells as determined by the transwell assay was not altered by miR-33a transfection (Fig. 8, *C* and *D*). Therefore, we focused the subsequent studies on the relevance of the TTF-1 → miR-33a ⊣ HMGA2 axis to cellular motility. The assumption was that miR-33a could functionally replace TTF-1 in slowing migration due to repression of HMGA2, which promotes cell motility (31). The murine 394T4-shLuc cells (Ttf-1^{high}), transfected with a mmu-miR-33 inhibitor (anti-miR-33a) or a negative control, were evaluated for migratory potential using the transwell assays. The anti-miR-33a conferred an increase in migration by 1.8-fold (Fig. 9*A*), indicating that derepression of Hmga2 by anti-miR-33a enhances cellular migration. Conversely, enforced overexpression of Hmga2 in the 394T4-shLuc cells increased its motility (Fig. 9*B*, *lane 1 versus lane 2*), phenocopying the cellular responses to anti-miR-33a. Transfection of the miR-33a mimic into 394T4-shLuc cells slowed down cellular motility, as shown in Fig. 9*B* (*lane 1 versus lane 3*). Importantly, stable overexpression of *Hmga2* lacking 3′-UTR overcame the inhibitory effect of miR-33a on cellular migration (Fig. 9*B*, *lane 3 versus lane 4*).

To complement these observations derived from the mouse lung cancer cells, we turned to the human NCI-H1299 cells, which are TTF-1^{low}. A human *HMGA2* cDNA lacking 3′-UTR and thus non-targetable by miR-33a was retrovirally transduced into NCI-H1299 cells for stable expression. Subsequently, either an miR-33a mimetic oligonucleotide or a scrambled control RNA oligonucleotide was introduced via transfection. RT-QPCR analysis showed that miR-33a mimic reduced the endogenous *HMGA2* RNA by 64% in NCI-H1299 cells (Fig. 9*C*). By the transwell assay, the miR-33a mimic transfection conferred a 40% reduction in motility of NCI-H1299 cells compared with a scrambled oligonucleotide (Fig. 9*D*, *lane 1 versus lane 3*). Importantly, this miR-33a-induced decrease in motility was rescued by the stable expression of the *HMGA2* transgene (Fig. 9*D*, *lane 3 versus lane 4*). These data implicate HMGA2 as a major mediator of miR-33a-directed impediment of lung cancer cell migration.

DISCUSSION

The study of Winslow *et al.* reported that *TTF-1*-dependent suppression of *HMGA2* is critical to the antimetastatic function

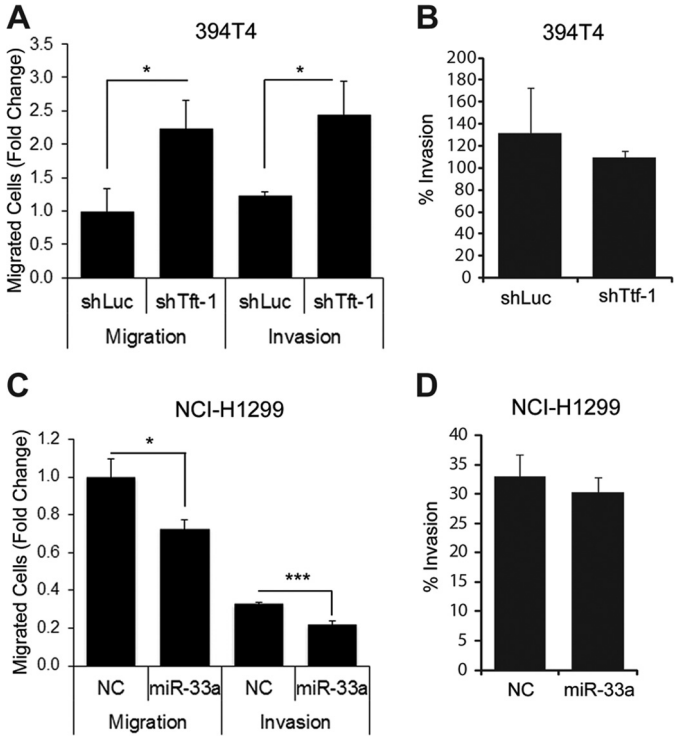

FIGURE 8. **Knockdown of endogenous Ttf-1 and exogenous miR-33a slow migration but do not alter invasiveness.** *A*, murine 394T4-shLuc and shTtf-1 cells were allowed to migrate through a membrane with 8-μm pores (*Migration*) or a membrane with 8-μm pores coated with Matrigel (*Invasion*) for 22 h. *B*, data from *A* were used to calculate the percentage invasion (% invasion = (mean number of cells invaded through the Matrigel-coated membrane)/(mean number of cells invaded through the uncoated membrane)). *C* and *D*, experiments here were conducted as in *A* and *B* except that NCI-H1299 cells transfected with a negative control oligonucleotide (*NC*) or an miR-33a mimic oligonucleotide were analyzed. *Error bars*, S.D. *, $p < 0.05$; ***, $p < 0.001$.

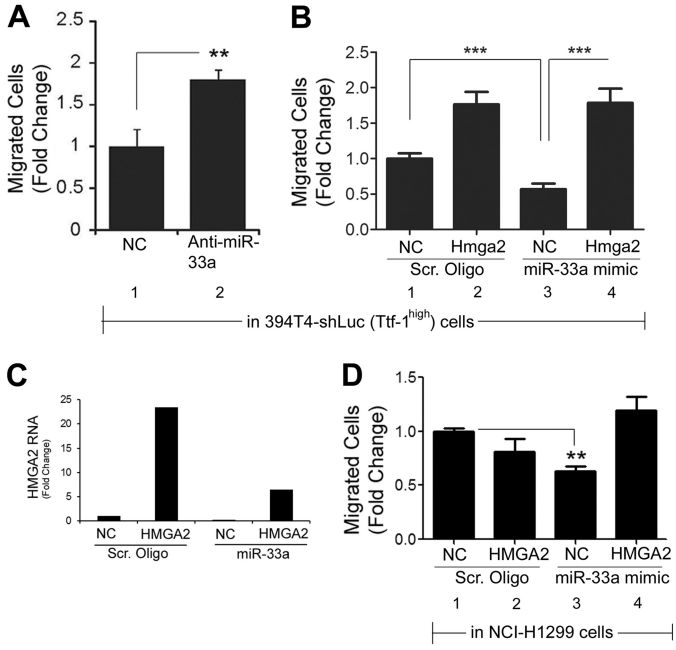

FIGURE 9. **The *TTF-1* → miR-33a ⊣ *HMGA2* signaling axis inhibits motility of lung cancer cells.** *A*, the murine 394T4-shLuc (Ttf-1^{high}) cells were transfected with a negative control oligonucleotide (*NC*) or an miR-33 inhibitor (anti-miR-33a) and allowed to migrate through uncoated transwell inserts for 22 h. Migrated cells were counted and normalized to negative control ($n = 3$). *B*, the murine 394T4-Ttf-1 cells stably expressing a transgene *Hmga2* lacking 3′-UTR were transfected with a scrambled control oligonucleotide (*Scr Oligo*) or an miR-33a mimetic oligonucleotide (*miR-33a mimic*). A transwell migration assay was performed as in *A*. *C*, RT-QPCR analysis of *HMGA2* RNA expression of NCI-H1299 transfectant cells. Human *HMGA2* was stably expressed via retrovirus-mediated gene transfer. Subsequently, a scrambled control oligonucleotide or an miR-33a mimetic oligonucleotide was transfected, and the RNA of total *HMGA2* (endogenous plus exogenous) was quantified by RT-QPCR. *D*, the human NCI-H1299 cells stably expressing a transgene *HMGA2* lacking 3′-UTR were transfected with a scrambled control oligonucleotide or an miR-33a mimetic oligonucleotide (miR-33a mimic). Transwell migration assay was performed as in *A*. *Error bars*, S.D. **, $p < 0.01$; ***, $p < 0.001$.

of *TTF-1* (24). In that study, the potential involvement of miRNAs in *Ttf-1*-driven suppression of *Hmga2* was focused on the let-7 family of miRNAs because of the known target/miRNA relationship between *HMGA2* and let-7s (13–15). Using a reporter plasmid that reads out let-7 activity, the primary and metastatic *Kras*$^{G12D/+}$;*p53*$^{\Delta/\Delta}$ mouse lung cancer cells of different Ttf-1 expression status exhibited equivalent let-7 activity, suggesting that the let-7 miRNAs do not intervene in the *Ttf-1*-directed *Hmga2* repression. However, considering the long 3′-UTR (~3 kb) of *HMGA2*/*Hmga2*, we hypothesized that other miRNAs may be dispatched by *Ttf-1* to repress *Hmga2*. Our earlier investigation identified the first miRNA (*i.e.* miR-365) that directly represses TTF-1 expression (27). This finding prompted us to initiate the present work to identify the miRNAs that are downstream to and directly regulated by TTF-1 using both loss- and gain-of-TTF-1-function strategies. A motivating factor was that the *TTF-1*-controlled miRNAs may target *HMGA2*, thus shedding mechanistic light on the *TTF-1* ⊣ *HMGA2* signaling axis. Therefore, our initial reverse (loss-of-function) screen via a QPCR array was *HMGA2* 3′-UTR-centric in that we compared the expression level of a series of miRNAs predicted to bind to *HMGA2* 3′-UTR in the Ttf-1^{low} and Ttf-1^{high} mouse lung cancer cell lines created by Winslow *et al.* (24). For the forward (gain-of-function) miRNA screen, we employed a TTF-1-inducible human lung cell system in which a *TTF-1*-transgene is under dox control (29). In this system, we conducted an unbiased global screen for miRNAs whose expression was altered from the TTF-1^{off} to TTF-1^{on} state using a commercial microarray bearing probes to all known human, mouse, and rat miRNAs. Interestingly, hsa-miR-33a/mmu-miR-33 was scored in both types of screens as an miRNA positively regulated by TTF-1. Curiously, miR-32 was also identified in the global forward screen as an miRNA that is up-regulated by TTF-1. Indeed, by chromatin immunoprecipitation, TTF-1 was demonstrated to bind to the promoter region of the host genes of both miR-33a and miR-32. However, only miR-33a was validated as a genuine miRNA that targets *HMGA2*. Clearly, the functional consequences of the TTF-1 → miR-32 regulation remain to be determined. Considering the documented expression alterations of miR-32 in lung cancer (down-regulation (42)), multiple myeloma (up-regulation (43)), and prostate cancer (up-regulation (44)), it is likely that miR-32 may also relay functionally significant signaling from TTF-1 in lung cancer.

The regulation of *HMGA2* is complex. For example, loss of the gastrointestinal transcription factor *Hnf4a* causes derepression of *Hmga2* in the Ttf-1-negative murine lung tumors (26). The data presented in this study unequivocally establish that

TTF-1 relies on miR-33a to hold *HMGA2* in check. This mode of restraining the *HMGA2* oncogene in lung cells appears conserved from mice to humans per our observations. In our experimental systems, it appears that miR-33a represents an important mediator of *TTF-1*-induced *HMGA2* repression in view of our "add-back" experiment (Fig. 6*C*) in which the endogenous *Hmga2* suppression imposed by the exogenous human *TTF-1* in the background of Ttf-1^{low} mouse cells (394T4-shTtf-1) was fully abolished by anti-miR-33a. However, it remains to be investigated whether TTF-1 may directly or indirectly influence HMGA2 expression via an miR-33a-independent manner, as suggested by Winslow *et al.* (24). Together with our recent finding of miR-365 directly targeting *TTF-1* (27), we believe that *TTF-1* can be unambiguously placed in the context of an miRNA-based network, with both up- and downstream microRNA signaling partners (miR-365 ⊣ *TTF-1* → miR-33a ⊣ *HMGA2*). Given the fact that TTF-1 is crucial to lung and thyroid development (45, 46), the miRNA network linked to TTF-1 will undoubtedly be shown to play a critical role in the development of these organs in the future.

TTF-1 joins an expanding list of cancer genes, such as *MDM2* (47), *NOTCH* (48), and *WT1* (49), displaying both pro- and antitumorigenic activities. This functional dimorphism is perhaps not surprising from the viewpoint that gene activities vary with genetic context. Established oncogenes like *AKT1* and *MYC* have also been shown to inhibit cancer invasion and metastasis (50, 51). Recently, we uncovered that TTF-1 directly transactivates epithelial tight junction genes, *OCCLUDIN* and *CLAUDIN-1*, impeding lung cancer cell motility and inducing anoikis (29). This suggests that the antimetastatic activity of *TTF-1* may be multipronged in several molecules. Consistent with this thesis, TTF-1 has been shown to reduce cell motility via transactivating *MYBPH* (52) and antagonizing TGFβ-induced EMT (39). In this study, the prominent phenotype of miR-33a overexpression is also on a metastasis-related phenotype, cell motility. It is curious that TTF-1 would invoke both transcriptional and post-transcriptional (miRNA) mechanisms to restrain lung cell migratory capacity. On the flip side, our findings beg the question of whether miRNAs also manifest the pro-oncogenic function of TTF-1.

In humans, there are two highly conserved miR-33 species (hsa-miR-33a and hsa-miR-33b). These two mature miRNAs differ by two nucleotides. However, in mice, there is a single species, mmu-miR-33, which is identical to hsa-miR-33a. In 2010, it was discovered that hsa-miR-33a is embedded in the 16th intron of *SREBF2*, and hsa-miR-33b is embedded in the 17th intron of *SREBP1* (53, 54). This new metabolism regulator, hsa-miR-33a, acts in concert with SREBP2 (the protein product of *SREBF2*) to supervise cholesterol homeostasis (53, 54), whereas SREBP2 has long been known as a master regulator of cholesterol metabolism, directly controlling the expression of many key enzymes along the cholesterol biosynthetic pathway (55, 56). In view of the data herein, one must ask if TTF-1 influences cholesterol homeostasis regionally in the lung. Furthermore, because *ABCA1*, a cholesterol exporter and a direct target of miR-33a (53, 54), displays anti-cancer activity (57), we postulate that cholesterol metabolism may be an integral and indispensable component of the pro- and/or antitumorigenic activities of *TTF-1*. Motivated by the finding that miR-33a targets the *PIM-1* oncogene (58), Ibrahim *et al.* (59) obtained positive data for an miR-33a replacement therapy in a model of colon carcinoma. Seeing the increasing cancer target multiplicity of miR-33a (*HMGA2* (this study), *PIM-1* (58), *CDK6* (60), *CCND1* (60), *PTHrP* (61), and *ABCA1* (53, 54)), we suggest that miR-33a acts as a liaison interfacing cholesterol homeostasis and tumorigenesis. In the future, it will be exciting to define the roles of the miRNA network in coupling the two processes.

Acknowledgments—We thank Dr. Jian-Jun Wei for the HMGA2 cDNA and Dr. Marcus Peter for the HMGA2 3′-UTR reporter construct.

REFERENCES

1. Bartel, D. P. (2004) MicroRNAs. Genomics, Biogenesis, Mechanism, and Function. *Cell* **116,** 281–297
2. Croce, C. M. (2009) Causes and consequences of microRNA dysregulation in cancer. *Nat. Rev. Genet.* **10,** 704–714
3. Esquela-Kerscher, A., and Slack, F. J. (2006) Oncomirs. MicroRNAs with a role in cancer. *Nat. Rev. Cancer* **6,** 259–269
4. He, L., and Hannon, G. J. (2004) MicroRNAs: small RNAs with a big role in gene regulation. *Nat. Rev. Genet.* **5,** 522–531
5. Bhaskaran, M., Wang, Y., Zhang, H., Weng, T., Baviskar, P., Guo, Y., Gou, D., and Liu, L. (2009) MicroRNA-127 modulates fetal lung development. *Physiol. Genomics* **37,** 268–278
6. Lizé, M., Herr, C., Klimke, A., Bals, R., and Dobbelstein, M. (2010) MicroRNA-449a levels increase by several orders of magnitude during mucociliary differentiation of airway epithelia. *Cell Cycle* **9,** 4579–4583
7. Sozzi, G., Pastorino, U., and Croce, C. M. (2011) MicroRNAs and lung cancer. From markers to targets. *Cell Cycle* **10,** 2045–2046
8. Yu, S. L., Chen, H. Y., Chang, G. C., Chen, C. Y., Chen, H. W., Singh, S., Cheng, C. L., Yu, C. J., Lee, Y. C., Chen, H. S., Su, T. J., Chiang, C. C., Li, H. N., Hong, Q. S., Su, H. Y., Chen, C. C., Chen, W. J., Liu, C. C., Chan, W. K., Chen, W. J., Li, K. C., Chen, J. J., and Yang, P. C. (2008) MicroRNA signature predicts survival and relapse in lung cancer. *Cancer Cell* **13,** 48–57
9. Dong, J., Jiang, G., Asmann, Y. W., Tomaszek, S., Jen, J., Kislinger, T., and Wigle, D. A. (2010) MicroRNA networks in mouse lung organogenesis. *PLoS One* **5,** e10854
10. Ventura, A., Young, A. G., Winslow, M. M., Lintault, L., Meissner, A., Erkeland, S. J., Newman, J., Bronson, R. T., Crowley, D., Stone, J. R., Jaenisch, R., Sharp, P. A., and Jacks, T. (2008) Targeted deletion reveals essential and overlapping functions of the miR-17 through 92 family of miRNA clusters. *Cell* **132,** 875–886
11. Tian, Y., Zhang, Y., Hurd, L., Hannenhalli, S., Liu, F., Lu, M. M., and Morrisey, E. E. (2011) Regulation of lung endoderm progenitor cell behavior by miR302/367. *Development* **138,** 1235–1245
12. Boyerinas, B., Park, S. M., Hau, A., Murmann, A. E., and Peter, M. E. (2010) The role of let-7 in cell differentiation and cancer. *Endocr. Relat. Cancer* **17,** F19–F36
13. Lee, Y. S., and Dutta, A. (2007) The tumor suppressor microRNA let-7 represses the HMGA2 oncogene. *Genes Dev.* **21,** 1025–1030
14. Mayr, C., Hemann, M. T., and Bartel, D. P. (2007) Disrupting the pairing between let-7 and Hmga2 enhances oncogenic transformation. *Science* **315,** 1576–1579
15. Park, S.-M., Shell, S., Radjabi, A. R., Schickel, R., Feig, C., Boyerinas, B., Dinulescu, D. M., Lengyel, E., and Peter, M. E. (2007) Let-7 prevents early cancer progression by suppressing expression of the embryonic gene *HMGA2*. *Cell Cycle* **6,** 2585–2590
16. Qi, J., and Mu, D. (2012) MicroRNAs and lung cancers. From pathogenesis to clinical implications. *Front. Med.* **6,** 134–155
17. Maeda, Y., Davé, V., and Whitsett, J. A. (2007) Transcriptional control of lung morphogenesis. *Physiol. Rev.* **87,** 219–244
18. Kendall, J., Liu, Q., Bakleh, A., Krasnitz, A., Nguyen, K. C., Lakshmi, B.,

Gerald, W. L., Powers, S., and Mu, D. (2007) Oncogenic cooperation and coamplification of developmental transcription factor genes in lung cancer. *Proc. Natl. Acad. Sci. U.S.A.* **104,** 16663–16668
19. Kwei, K. A., Kim, Y. H., Girard, L., Kao, J., Pacyna-Gengelbach, M., Salari, K., Lee, J., Choi, Y. L., Sato, M., Wang, P., Hernandez-Boussard, T., Gazdar, A. F., Petersen, I., Minna, J. D., and Pollack, J. R. (2008) Genomic profiling identifies TITF1 as a lineage-specific oncogene amplified in lung cancer. *Oncogene* **27,** 3635–3640
20. Tanaka, H., Yanagisawa, K., Shinjo, K., Taguchi, A., Maeno, K., Tomida, S., Shimada, Y., Osada, H., Kosaka, T., Matsubara, H., Mitsudomi, T., Sekido, Y., Tanimoto, M., Yatabe, Y., and Takahashi, T. (2007) Lineage-specific dependency of lung adenocarcinomas on the lung development regulator TTF-1. *Cancer Res.* **67,** 6007–6011
21. Weir, B. A., Woo, M. S., Getz, G., Perner, S., Ding, L., Beroukhim, R., Lin, W. M., Province, M. A., Kraja, A., Johnson, L. A., Shah, K., Sato, M., Thomas, R. K., Barletta, J. A., Borecki, I. B., Broderick, S., Chang, A. C., Chiang, D. Y., Chirieac, L. R., Cho, J., Fujii, Y., Gazdar, A. F., Giordano, T., Greulich, H., Hanna, M., Johnson, B. E., Kris, M. G., Lash, A., Lin, L., Lindeman, N., Mardis, E. R., McPherson, J. D., Minna, J. D., Morgan, M. B., Nadel, M., Orringer, M. B., Osborne, J. R., Ozenberger, B., Ramos, A. H., Robinson, J., Roth, J. A., Rusch, V., Sasaki, H., Shepherd, F., Sougnez, C., Spitz, M. R., Tsao, M. S., Twomey, D., Verhaak, R. G., Weinstock, G. M., Wheeler, D. A., Winckler, W., Yoshizawa, A., Yu, S., Zakowski, M. F., Zhang, Q., Beer, D. G., Wistuba, I. I., Watson, M. A., Garraway, L. A., Ladanyi, M., Travis, W. D., Pao, W., Rubin, M. A., Gabriel, S. B., Gibbs, R. A., Varmus, H. E., Wilson, R. K., Lander, E. S., and Meyerson, M. (2007) Characterizing the cancer genome in lung adenocarcinoma. *Nature* **450,** 893–898
22. Watanabe, H., Francis, J. M., Woo, M. S., Etemad, B., Lin, W., Fries, D. F., Peng, S., Snyder, E. L., Tata, P. R., Izzo, F., Schinzel, A. C., Cho, J., Hammerman, P. S., Verhaak, R. G., Hahn, W. C., Rajagopal, J., Jacks, T., and Meyerson, M. (2013) Integrated cistromic and expression analysis of amplified NKX2–1 in lung adenocarcinoma identifies LMO3 as a functional transcriptional target. *Genes Dev.* **27,** 197–210
23. Yamaguchi, T., Yanagisawa, K., Sugiyama, R., Hosono, Y., Shimada, Y., Arima, C., Kato, S., Tomida, S., Suzuki, M., Osada, H., and Takahashi, T. (2012) NKX2–1/TITF1/TTF-1-induced ROR1 is required to sustain EGFR survival signaling in lung adenocarcinoma. *Cancer Cell* **21,** 348–361
24. Winslow, M. M., Dayton, T. L., Verhaak, R. G., Kim-Kiselak, C., Snyder, E. L., Feldser, D. M., Hubbard, D. D., DuPage, M. J., Whittaker, C. A., Hoersch, S., Yoon, S., Crowley, D., Bronson, R. T., Chiang, D. Y., Meyerson, M., and Jacks, T. (2011) Suppression of lung adenocarcinoma progression by Nkx2–1. *Nature* **473,** 101–104
25. Maeda, Y., Tsuchiya, T., Hao, H., Tompkins, D. H., Xu, Y., Mucenski, M. L., Du, L., Keiser, A. R., Fukazawa, T., Naomoto, Y., Nagayasu, T., and Whitsett, J. A. (2012) Kras(G12D) and Nkx2–1 haploinsufficiency induce mucinous adenocarcinoma of the lung. *J. Clin. Invest.* **122,** 4388–4400
26. Snyder, E. L., Watanabe, H., Magendantz, M., Hoersch, S., Chen, T. A., Wang, D. G., Crowley, D., Whittaker, C. A., Meyerson, M., Kimura, S., and Jacks, T. (2013) Nkx2–1 represses a latent gastric differentiation program in lung adenocarcinoma. *Mol. Cell* **50,** 185–199
27. Qi, J., Rice, S. J., Salzberg, A. C., Runkle, E. A., Liao, J., Zander, D. S., and Mu, D. (2012) MiR-365 regulates lung cancer and developmental gene thyroid transcription factor 1. *Cell Cycle* **11,** 177–186
28. Bommer, G. T., and MacDougald, O. A. (2011) Regulation of lipid homeostasis by the bifunctional SREBF2-miR33a locus. *Cell Metab.* **13,** 241–247
29. Runkle, E. A., Rice, S. J., Qi, J., Masser, D., Antonetti, D. A., Winslow, M. M., and Mu, D. (2012) Occludin is a direct target of thyroid transcription factor-1 (TTF-1/NKX2–1). *J. Biol. Chem.* **287,** 28790–28801
30. Shell, S., Park, S. M., Radjabi, A. R., Schickel, R., Kistner, E. O., Jewell, D. A., Feig, C., Lengyel, E., and Peter, M. E. (2007) Let-7 expression defines two differentiation stages of cancer. *Proc. Natl. Acad. Sci. U.S.A.* **104,** 11400–11405
31. Wu, J., Liu, Z., Shao, C., Gong, Y., Hernando, E., Lee, P., Narita, M., Muller, W., Liu, J., and Wei, J.-J. (2011) HMGA2 overexpression-induced ovarian surface epithelial transformation is mediated through regulation of EMT genes. *Cancer Res.* **71,** 349–359
32. Ritchie, M. E., Silver, J., Oshlack, A., Holmes, M., Diyagama, D., Holloway, A., and Smyth, G. K. (2007) A comparison of background correction methods for two-colour microarrays. *Bioinformatics* **23,** 2700–2707
33. Fusco, A., and Fedele, M. (2007) Roles of HMGA proteins in cancer. *Nat. Rev. Cancer* **7,** 899–910
34. Grimson, A., Farh, K. K., Johnston, W. K., Garrett-Engele, P., Lim, L. P., and Bartel, D. P. (2007) MicroRNA targeting specificity in mammals. Determinants beyond seed pairing. *Mol. Cell* **27,** 91–105
35. Reddel, R. R., Ke, Y., Gerwin, B. I., McMenamin, M. G., Lechner, J. F., Su, R. T., Brash, D. E., Park, J. B., Rhim, J. S., and Harris, C. C. (1988) Transformation of human bronchial epithelial cells by infection with SV40 or adenovirus-12 SV40 hybrid virus, or transfection via strontium phosphate coprecipitation with a plasmid containing SV40 early region genes. *Cancer Res.* **48,** 1904–1909
36. Hsu, D. S., Acharya, C. R., Balakumaran, B. S., Riedel, R. F., Kim, M. K., Stevenson, M., Tuchman, S., Mukherjee, S., Barry, W., Dressman, H. K., Nevins, J. R., Powers, S., Mu, D., and Potti, A. (2009) Characterizing the developmental pathways TTF-1, NKX2–8, and PAX9 in lung cancer. *Proc. Natl. Acad. Sci. U.S.A.* **106,** 5312–5317
37. Boggaram, V. (2009) Thyroid transcription factor-1 (TTF-1/Nkx2.1/TITF1) gene regulation in the lung. *Clin. Sci.* **116,** 27–35
38. Damante, G., Fabbro, D., Pellizzari, L., Civitareale, D., Guazzi, S., Polycarpou-Schwartz, M., Cauci, S., Quadrifoglio, F., Formisano, S., and Di Lauro, R. (1994) Sequence-specific DNA recognition by the thyroid transcription factor-1 homeodomain. *Nucleic Acids Res.* **22,** 3075–3083
39. Saito, R. A., Watabe, T., Horiguchi, K., Kohyama, T., Saitoh, M., Nagase, T., and Miyazono, K. (2009) Thyroid transcription factor-1 inhibits transforming growth factor-β-mediated epithelial-to-mesenchymal transition in lung adenocarcinoma cells. *Cancer Res.* **69,** 2783–2791
40. Guazzi, S., Price, M., De Felice, M., Damante, G., Mattei, M. G., and Di Lauro, R. (1990) Thyroid nuclear factor 1 (TTF-1) contains a homeodomain and displays a novel DNA binding specificity. *EMBO J.* **9,** 3631–3639
41. Saetrom, P., Heale, B. S., Snøve, O., Jr., Aagaard, L., Alluin, J., and Rossi, J. J. (2007) Distance constraints between microRNA target sites dictate efficacy and cooperativity. *Nucleic Acids Res.* **35,** 2333–2342
42. Yanaihara, N., Caplen, N., Bowman, E., Seike, M., Kumamoto, K., Yi, M., Stephens, R. M., Okamoto, A., Yokota, J., Tanaka, T., Calin, G. A., Liu, C. G., Croce, C. M., and Harris, C. C. (2006) Unique microRNA molecular profiles in lung cancer diagnosis and prognosis. *Cancer Cell* **9,** 189–198
43. Pichiorri, F., Suh, S. S., Ladetto, M., Kuehl, M., Palumbo, T., Drandi, D., Taccioli, C., Zanesi, N., Alder, H., Hagan, J. P., Munker, R., Volinia, S., Boccadoro, M., Garzon, R., Palumbo, A., Aqeilan, R. I., and Croce, C. M. (2008) MicroRNAs regulate critical genes associated with multiple myeloma pathogenesis. *Proc. Natl. Acad. Sci. U.S.A.* **105,** 12885–12890
44. Ambs, S., Prueitt, R. L., Yi, M., Hudson, R. S., Howe, T. M., Petrocca, F., Wallace, T. A., Liu, C. G., Volinia, S., Calin, G. A., Yfantis, H. G., Stephens, R. M., and Croce, C. M. (2008) Genomic profiling of microRNA and messenger RNA reveals deregulated microRNA expression in prostate cancer. *Cancer Res.* **68,** 6162–6170
45. Antonica, F., Kasprzyk, D. F., Opitz, R., Iacovino, M., Liao, X. H., Dumitrescu, A. M., Refetoff, S., Peremans, K., Manto, M., Kyba, M., and Costagliola, S. (2012) Generation of functional thyroid from embryonic stem cells. *Nature* **491,** 66–71
46. Kimura, S., Hara, Y., Pineau, T., Fernandez-Salguero, P., Fox, C. H., Ward, J. M., and Gonzalez, F. J. (1996) The T/ebp null mouse. Thyroid-specific enhancer-binding protein is essential for the organogenesis of the thyroid, lung, ventral forebrain, and pituitary. *Genes Dev.* **10,** 60–69
47. Manfredi, J. J. (2010) The Mdm2-p53 relationship evolves. Mdm2 swings both ways as an oncogene and a tumor suppressor. *Genes Dev.* **24,** 1580–1589
48. Radtke, F., and Raj, K. (2003) The role of Notch in tumorigenesis. Oncogene or tumour suppressor? *Nat. Rev. Cancer* **3,** 756–767
49. Yang, L., Han, Y., Suarez Saiz, F., and Minden, M. D. (2007) A tumor suppressor and oncogene. The WT1 story. *Leukemia* **21,** 868–876
50. Liu, H., Radisky, D. C., Nelson, C. M., Zhang, H., Fata, J. E., Roth, R. A., and Bissell, M. J. (2006) Mechanism of Akt1 inhibition of breast cancer cell invasion reveals a protumorigenic role for TSC2. *Proc. Natl. Acad. Sci.*

U.S.A. **103,** 4134–4139
51. Liu, H., Radisky, D. C., Yang, D., Xu, R., Radisky, E. S., Bissell, M. J., and Bishop, J. M. (2012) MYC suppresses cancer metastasis by direct transcriptional silencing of α_v and β_3 integrin subunits. *Nat. Cell Biol.* **14,** 567–574
52. Hosono, Y., Yamaguchi, T., Mizutani, E., Yanagisawa, K., Arima, C., Tomida, S., Shimada, Y., Hiraoka, M., Kato, S., Yokoi, K., Suzuki, M., and Takahashi, T. (2012) MYBPH, a transcriptional target of TTF-1, inhibits ROCK1, and reduces cell motility and metastasis. *EMBO J.* **31,** 481–493
53. Moore, K. J., Rayner, K. J., Suárez, Y., and Fernández-Hernando, C. (2011) The role of microRNAs in cholesterol efflux and hepatic lipid metabolism. *Annu. Rev. Nutr.* **31,** 49–63
54. Rottiers, V., and Näär, A. M. (2012) MicroRNAs in metabolism and metabolic disorders. *Nat. Rev. Mol. Cell Biol.* **13,** 239–250
55. Brown, M. S., and Goldstein, J. L. (1997) The SREBP pathway. Regulation of cholesterol metabolism by proteolysis of a membrane-bound transcription factor. *Cell* **89,** 331–340
56. Horton, J. D., Goldstein, J. L., and Brown, M. S. (2002) SREBPs. Activators of the complete program of cholesterol and fatty acid synthesis in the liver. *J. Clin. Invest.* **109,** 1125–1131
57. Smith, B., and Land, H. (2012) Anticancer activity of the cholesterol exporter ABCA1 gene. *Cell Rep.* **2,** 580–590
58. Thomas, M., Lange-Grünweller, K., Weirauch, U., Gutsch, D., Aigner, A., Grünweller, A., and Hartmann, R. K. (2012) The proto-oncogene Pim-1 is a target of miR-33a. *Oncogene* **31,** 918–928
59. Ibrahim, A. F., Weirauch, U., Thomas, M., Grünweller, A., Hartmann, R. K., and Aigner, A. (2011) MicroRNA replacement therapy for miR-145 and miR-33a is efficacious in a model of colon carcinoma. *Cancer Res.* **71,** 5214–5224
60. Cirera-Salinas, D., Pauta, M., Allen, R. M., Salerno, A. G., Ramírez, C. M., Chamorro-Jorganes, A., Wanschel, A. C., Lasuncion, M. A., Morales-Ruiz, M., Suarez, Y., Baldan, Á., Esplugues, E., and Fernández-Hernando, C. (2012) Mir-33 regulates cell proliferation and cell cycle progression. *Cell Cycle* **11,** 922–933
61. Kuo, P. L., Liao, S. H., Hung, J. Y., Huang, M. S., and Hsu, Y. L. (2013) MicroRNA-33a functions as a bone metastasis suppressor in lung cancer by targeting parathyroid hormone related protein. *Biochim. Biophys. Acta* **1830,** 3756–3766